GEOLOGICAL SURVEY OF CANADA

OPEN FILE 3868

Neotectonic mapping of eastern Juan de Fuca Strait, Cascadia forearc region: initial results

D.C. Mosher

2001

Natural Resources Canada | Ressources naturelles Canada

Canada

NEOTECTONIC MAPPING OF EASTERN JUAN DE FUCA STRAIT, CASCADIA FOREARC REGION: INITIAL RESULTS

Geological Survey of Canada Open File Report 3868

David C. Mosher

Geological Survey of Canada - Pacific
9860 West Saanich Rd.,
Box 6000, Sidney, BC
Canada
V8L 4B2

"Research supported by the U.S. Geological Survey (USGS), Department of the Interior, under USGS award number 1434-HQ-96-GR-02726. The views and conclusions contained in this document are those of the authors and should not be interpreted as necessarily representing the official policies, either expressed or implied, of the U.S. Government."

NEOTECTONIC MAPPING OF EASTERN JUAN DE FUCA STRAIT, CASCADIA FOREARC REGION: INITIAL RESULTS

David C. Mosher

Geological Survey of Canada - Pacific
P.O. Box 6000,
Sidney, BC
Canada
V8L 4B2

Abstract

The area of eastern Juan de Fuca Strait spans a concentration of modern crustal seismicity, which extends northwards from Puget Sound. The region lies in a north-south compressional tectonic regime in addition to a west-east subduction setting. Although many earthquakes have been recorded in this area in modern times, there has been little evidence of any geologic expression of them or their Quaternary counterparts. Geologic evidence of earthquakes, e.g. recent faulting, however, can provide important information on earthquake hazard.

Two regional systematic marine geophysical surveys of the eastern Juan de Fuca Strait have been completed. Over 2200 line- km of multi- and single channel seismic reflection data were collected along with 39 shallow piston- and vibro-cores during the two surveys. Geophysical data show widespread evidence of faulting. In the shallow, unconsolidated sediment section, this evidence is interpreted as 1) normal growth faults with offsets on the order of metres, and 2) sediment deformation features with "dropouts" on the order of tens of metres. These deformation features occur in zones, typically several kilometres wide, which broadly correlate with known and projected Tertiary and younger fault systems mapped on land and from previous marine surveys. Specifically, the Leech River/ Southern Whidbey Island fault, the Devil's Mountain fault, the Hood Canal-Discovery Bay fault are readily identified from mapping these features. Deformation features can be seen on seismic reflection profiles to overlie fault offsets in basement rocks. Basement faults are observed to be normal, thrust and reverse-normal faults, sometimes throwing Tertiary basement rock over glacial sediments. Throw on these faults can be on the order of tens of metres. In most cases, observed faults or related deformation features cut through or affect the entire late Pleistocene glacial marine sedimentary section. In a few instances, these features extend into the Holocene, although the Holocene section is typically thin, highly reworked and extremely variable in age and sediment type. Accurate dating of piston core samples will better constrain the age of latest displacements. The abundant evidence of recent faulting (since deglaciation) in an area of active seismicity is highly relevant to the assessment of earthquake hazard in the region.

Introduction

The area of eastern Juan de Fuca Strait spans a concentration of modern crustal seismicity which extends northwards from Puget Sound. In modern history, some of these earthquakes have been damaging (e.g. southern Puget Sound, 1949 and 1965). The most recent notable event occurred north of Seattle in May, 1996 with a M5.4 (centered in Duvall). The region lies in a north-south compressional tectonic regime in addition to a west-east subduction setting. Although many earthquakes have been recorded in this area in modern times, there has been little evidence of any geologic expression of them or their Quaternary counterparts. Geologic evidence of earthquakes, e.g. recent faulting, however, can provide important information on earthquake hazard. Faulting is difficult to identify on land because of steep, rugged topography, heavy tree cover and subaerial erosion and weathering. In contrast, faults often can be readily recognized on and under the seafloor with acoustic imaging (seismic reflection and sidescan sonar). The objectives of the present program are to conduct an intensive geological/geophysical survey using multichannel and high resolution seismic reflection, sidescan sonar and piston coring to study, define and date the stratigraphy and evidence of neotectonic activity, such as earthquake-related faults, in the region. In addition, these data are relevant to the seismic hazard to adjacent urban centres, hazards to marine development and bear upon environmental and resource issues in these coastal waters.

Investigations Undertaken

Marine geophysical and geological investigations were conducted for this project during two research expeditions on the CCGS John P. Tully; cruise designations are PGC96006 and PGC97007. PGC96006 took place between October 15 and 3 1, 1996 and PGC97007 took place between August 5 and 16, 1997. A detailed and systematic grid of multi- and single channel seismic reflection lines were completed over the study area, totaling over 2100 line-km (Tables 1-4, and Fig. 1). In addition, 39 sediment cores (Table 5) were collected to provide geophysical groundtruth, establish a stratigraphic succession and provide material for age-dating (Table 6).

Methods

Seismic reflection

Multichannel seismic reflection (MCS), a tuned array of airgun single channel and Huntec high resolution subbottom profiles have been collected over the study area (Fig. 1). The multichannel system consisted of a Haliburton 0.65 l (40 in^3) sleeve gun and an Innovative Transducers Inc. (ITI) 24-channel hydrophone solid array. The array had 3 hydrophones per group and 8 m separation between the centre hydrophone in each group. Separation between the gun and the centre element of the first group was 56 m. The streamer and gun were towed at 1 m below the sea surface. The gun was fired every 16 m using differential GPS to calculate the offset from the last shot. The sleeve gun was charged with a Rix air compressor capable of 30 standard cubic feet per minute, which maintained a pressure in the gun of about 2000 psi.

MCS data were digitized with a Geometrics StrataView© acquisition system with a sample interval of 500 µs over a record length of 2048 ms. This sample rate translates to a Nyquist frequency of 1000 Hz, well in excess of the bandwidth of the 40 in^3 source. The centre frequency of the source is about 150 Hz and the bandwidth extends from 0 to about 400 Hz. Data were written to an external SCSI hard drive, then archived to

EXABYTE™ tape in SEG-2 format. Data were then downloaded to a HP 715 work station, converted to SEG-Y format, merged with navigation data, collated into line segments and processed. Trace data from channel 5 were extracted and printed. The configuration of the array allowed for a six-fold common depth point (CDP) stack of the data. Initial stacks with semblance velocity analysis were conducted on board the vessel during the survey. For this processing, the data were subsampled to 1 ms sample interval, with no loss of information, and terminated at a record length of 1024 ms.

The Huntec Deep Tow System was employed continuously during all surveying through both PGC96006 and PGC97007. It was maintained by Geoforce Consultants Ltd., and operated by Geoforce and Pacific Geoscience Centre staff. The system uses a boomer source with an internal and external hydrophone receiving array. The ED lOG/C boomer source generates a broad band pulse with a centre frequency of about 2.5 kHz, but spans 0.5 to 6 kHz relatively cleanly. The system was operated at 500 Joules output. This source is highly repeatable, capable of resolving 10 cm vertically. Peak output intensity is 118 dB relative to 1 microbar at 1 metre, with a pulse duration of 120 microseconds. It was deep-towed between 30 and 60 m below the surface in this survey. Deep towing the system puts the source and receiver closer to the seafloor and away from surface heave. The system is depth and heave compensated. The internal hydrophone is a LC32 single element cartridge suspended from the boomer plate and is best for high frequency acquisition. The external array is a 15 ft-long, 10-element oil filled streamer (Benthos MESH lS/lOP) towed behind the fish. It acquires a broader frequency band than the internal hydrophone, but is subject to heave and more external noise. The internal and external signals were displayed in analogue hardcopy on an EPC9800 thermal chart recorder, recorded on a Sony™ DAT 9-channel recorder and were digitized at 40 μs for a record length of 175 ms (deep-water delays were used to keep the record length short) and written to EXABYTE tape with a MUSE@ digital sonar acquisition system. This sample interval yields a Nyquist frequency of 12.5 kHz. The boomer source was fired at every 1.5 m, but was interrupted during acquisition of the multi-channel data. The external data were band pass filtered at 800-6000 Hz.

Single channel seismic reflection data were collected during PGC97007. The seismic source consisted of two Bolt™ airguns with various chamber sizes (typically 10 in^3) suspended in a frame, 0.5 m apart and towed at a depth of 0.5 m and 15 m behind the stern of the ship. Airguns were pressurized to 1850 psi and fired every 4 m, based on differential GPS positioning. A single ED0 model 141B hydrophone cartridge was deep-towed below the airguns to monitor every shot signature. The relative timing of the firing of the two guns was controlled by a 3-channel Bolt™ firing unit, permitting 0.1 ms accuracy in firing delay. The shot point source signature was monitored on a Zonic model 3525 spectral analyzer. The shot point hydrophone and analyzer provided real-time display of the source signature in the time and frequency domains. The source signature was then tuned to optimize the outgoing pulse for shape and frequency content by adjusting the relative firing time of the two guns.

Two hydrophone streamers were used to acquire the single channel seismic reflection data. 1) A Benthos array, which is oil-filled and consists of a single group of 50 elements with 6 inch spacing. It was towed just below the surface, 30 m behind the ship; and 2) A Teledyne array, which has a 25 m active section with 50 hydrophone cartridges. It was towed at 3 m depth, 50 m behind the ship. Signal from these arrays and the single

cartridge shot point hydrophone were displayed as analogue hardcopy on an EPC 9800 chart recorder, logged to a SONY™ DAT recorder and digitized at 100 μs for a length of 1000 ms on EXABYTE™ tape with a MUSE© digital sonar acquisition system.

Sidescan Sonar

The sidescan sonar system used was a Simrad 992. It is a dual frequency system (120 and 330 kHz) set at 300 m range (300 m per side) for this survey. Data were output to an Alden™ 9315 continuous tone greyscale printer and were digitized at 2048 samples per side with the MUSE© acquisition system. The sidescan fish was towed about 30 m above the seafloor with a 157 kg depressor.

Bathymetry

Water depth data, acquired through a hull-mounted Simrad™ EA500 12 kHz sounder, were logged continuously at five second intervals with navigation data during the two cruises. In addition, digital Canadian Hydrographic Service (CHS) and NOAA data were obtained and field sheet data were digitized. A swath bathymetry survey was conducted along the Victoria water front in September, 1998 and these data have been combined with the other data.

Sediment Coring

Seventeen piston cores were collected or attempted during PGC96006 and a further 22 piston cores and 4 vibrocores were collected during PGC97007 (Table 5). For the piston cores, a standard Benthos™ split-piston corer was used with a 2000 lb core head and two 3.3 m (10 ft) barrels. Cores are recovered inside a plastic liner, which has an internal diameter of 2.5 inches. Cores were sealed and kept in refrigerated storage. The vibrocorer had limited success due to steep terrain. Cores have been split and described and measured for physical properties (porosity, density, micro-resistivity, acoustic velocity, and shear strength). This project spawned the need and has resulted in the establishment of a physical properties laboratory at the Pacific Geoscience Centre.

Navigation

Navigation acquisition and post-processing were provided by Geoforce Consultants Ltd. Position data were acquired every 1 second using the differential Global Positioning System (DGPS). The differential signal was acquired from Whidbey Island or Race Rocks stations and was stable throughout the survey, although some post-processing is still necessary. The navigation receiver was a Trimble™ 6-channel receiver. The GPS receiving antenna was mounted on the after mast of the CCGS John P. Tully, 15.3 m from the fantail. In addition, to our own position data, the ship's navigation was acquired, which operates through antennae on the main mast and displays data in NAD27 datum, while ours was in NAD83. All data were acquired digitally and logged to hard drive.

Results and Discussion

All data collected and interpreted are digital and the interpreted data have been loaded into ARC/Info©, a Geographic Information System (GIS) software package. These data have been merged with land topographic, coastline, cultural and existing digital geophysical data to produce a series of maps that can be integrated at equivalent scales.

Regional Potential Field Maps

Existing regional geophysical data include shipborne gravity and airborne magnetic data. These data show two main geologic bedrock members; the high gravity, highly magnetic Crescent Terrane volcanic and crystalline rocks to the west, and the low gravity, low magnetic Pacific Rim Terrane sedimentary rocks to the east. The magnetic data (Fig. 2) show the contact between the two terranes with sharp contrasts in magnetic signatures representing regional faults, such as the Leech River (south Whidbey Island) and Sooke Basin (Hood Canal) fault zones, as well as the Trial Island and Devil's Mountain faults. These data provide the framework for the more detailed investigations.

Surveys

Tables 1 to 5 and Figure 1 summarize the lines run with the three seismic systems and core locations in the survey area. 1350 line-km of multichannel seismic (MCS) data, and Huntec high resolution reflection data were collected in 1996 in a largely east-west grid with one nautical mile line spacing. 850 line-km of single channel seismic reflection (SCS) and Huntec high resolution reflection data were collect in 1997. This grid orientation was largely northeast-southwest. 39 piston and vibrocores (Table 5) were collected to provide groundtruth for the geophysical interpretations and to collect material for ^{14}C-dating. Coring targets included the different seismic facies encountered, as well as the stratigraphic successions in order to establish the Quaternary stratigraphy. Specific features such as faults or reflectors which intersected faults were also targeted.

Bathymetry

A bathymetric image of the study area is shown in Figure 3. Water depths range to a maximum of about 250 m. The area has a number of shallow banks, some of which are supratidal, with intervening deep troughs. The most significant trough cuts southwest through the center of the study area at about the same location as the contact between the two underlying bedrock terranes. The gross morphology is believed to reflect the glacial/postglacial surface, with little modification through the Holocene. Bedforms of various scales are observed on the seafloor, indicative of the dynamic current regime that presently exists in the region.

Quaternary Geology

High resolution seismic reflection data show four seismic units believed to represent three distinct near-surface geologic units. Interpretations are based on geophysical correlation with sediment cores descriptions and shoreline outcrops. Physical property measurements in the cores have been used as a correlation tool as well. Unit 1 is bedrock, as interpreted from the nature of internal reflectors and high amplitude surface reflections. The base of the Quaternary section has been digitally "picked" and its surface morphology is shown in Figure 4. This horizon is essentially the contact between bedrock and unlithified Quaternary sediment. Above this horizon, the next stratigraphic unit (Unit 2) is acoustically amorphous and attenuates the acoustic signal so no high resolution information is collected below it. Its surface varies considerably in depth, and usually outcrops or comes close to surface on the bank tops (Fig. 5). It is believed to represent till and/or diamict, likely deposited by ice from the most recent glacial episode (Fraser stade). This unit is overlain in a conformable fashion by acoustically stratified sediment package (Unit 3) that is up to 50 m thick (Fig. 5). It is believed to be a glacial marine section deposited during the recession of the last glaciation. The surface of this unit is

frequently eroded, thus the topmost unit lies unconformably on this glacial marine unit. The topmost unit (Unit 4) represents Holocene deposition and is composed of reworked glacial and glacial marine sediments (Fig. 5). Its thickness varies from 0 to 30 m. It is finely bedded with abundant sedimentary bedforms internally and on the seabed.

A surficial geology map has been generated from an interpretation of high resolution seismic reflection data, combined with results from coring to provide groundtruth (Fig. 6). This map shows the various units outcropping at the seafloor. Bedrock (Unit 1) is exposed only near the coastline. Till and/or diamict (Unit 2) comprise the shallow banks. Glaciomarine sediments (Unit 3) form the majority of the seafloor in the western regions of the study area. Holocene reworked material (Unit 4) is more prevalent to the east; largely representing sediment supply from vast deposits of Pleistocene sediments on Whidbey Island.

Neotectonics

Seismic reflection profiles show evidence of faulting in bedrock and, occasionally, within the unconsolidated sediment section (Figs. 7 and 8). More common in the unconsolidated sediment section, however, are sediment deformation features (Figs. 9 and 10). There is strong suggestion that these deformation features correlate with basement faulting, at least in some cases (see Figs. 10a&b). Figure 11 is a distribution map of faulting and sediment deformation features. Although are many such features in the study area, there are only slight indications of any correlation with faults mapped from magnetic data and land topography. These results suggest that faulting is active within the Holocene, sometimes affecting the present seafloor, but movement along the major crustal elements is not readily apparent from the shallow, near-surface faults and deformation features observed from the seismics. If there is movement on these structural elements then it is likely dispersed into zones of deformation. It must be noted, however, that the distribution of these features is biased to areas where the ship can travel and where seismic subbottom penetration is successful. For example, in some cases the bank tops are too shallow for a ship, and in many cases the banks represent areas where there is little subbottom penetration and abundant multiple interference.

Conclusions

The presence of fault offsets and deformation features in post-glacial sediments suggests that neotectonic activity has taken place within the Holocene. The exact timing of these offsets is not known but with core and seismic-stratigraphic data it should be possible to date some of these features. It is critical to establish the timing of these displacements in order to separate neotectonic activity resulting from present day tectonic stresses from post-glacial rebound activity. Mapping of the distribution of these features is not yet complete, but preliminary results suggest only small correlation with major terrain boundaries. The seemingly random distribution of seismicity and of mapped shallow faults and deformation features suggests that neotectonic activity in the region may not be taking place along the major terrane boundaries as a line of failure. It is more likely that failure is distributed throughout zones of deformation or in isolated basins and within smaller tectonic elements within the crust.

Acknowledgements

The author would like to thank the United States Geological Survey External Research Program of the National Earthquake Hazard Reduction Plan (NEHRP) for funding this project. The results included within this report would not have been possible were it not for the efforts of the officers, crew, and scientific staff of *CCGS John P. Tully* cruises PGC96006 and PGC97007. In particular, I would like to thank Captain John Anderson, with whom it was a pleasure to sail, and the rest of the bridge officers who maneuvered under heavy marine traffic conditions. R. Kung has compiled all the geo-referenced data within ArcInfo. His skills are much appreciated and have made this effort a "state-of-the-art" project. A. Hewitt conducted the digital horizon picking, split and described the piston cores and produced the surficial geology map. I thank R. Currie for critical reviews of this report. The data collection and curation efforts of PGC staff K. Conway, R. MacDonald, and W. Hill are very much appreciated.

Table 1: start and end times of all lines

PGC96006

Line	Start Time	End Time
1	290/2130	291/0650
2	291/0641	291/1536
3A	291/1602	291/1911
3B	292/0511	292/1217
4	292/1301	292/2122
5A	292/2154	293/0617
6	293/0657	293/1815
7	293/2015	294/0634
8A	294/0738	294/1043
8B	295/0531	295/1311
9A	294/1143	294/1546
9B	295/1437	295/2137
10	294/1604	294/1734
11	294/1836	295/0458
12	295/2213	296/0043
13	296/0058	296/0332
14	296/0338	296/1041
15	296/1202	296/1636
16	296/1711	296/1835
17	296/1844	296/2149
18	296/2152	296/2327
19	296/2335	297/0809
20	297/0809	297/0836
21	297/0836	297/1919
22	297/2019	297/2351
23	298/0015	298/0346
24	298/0406	298/0717
25	298/0800	298/1036
26	298/1036	298/1243
27	298/1258	298/1310
28	299/0130	299/0906
29	299/0938	299/1220
30	299/1252	299/1329
31	299/1408	299/1441
32	299/2209	300/0703
33	300/0841	300/1706
34	301/0207	301/0609
35	301/0615	301/1036
36	301/1042	301/1217
37	301/1221	301/1836
38	302/0049	302/0126
39	302/0142	302/0219
40	302/0320	302/0342
41	302/0504	302/0529
42	302/0613	302/0647
43	302/0851	302/0918
44	302/0930	302/1000
45	302/1016	302/1041
46	302/1113	302/1530
47	302/1554	302/1634
48	302/1634	302/1641
49	302/1641	302/1708
50	302/1708	302/1732
51	302/1732	302/1801
52	302/1801	302/1828
53	302/1828	302/1927
54	302/1927	302/1951
55	302/1951	302/?
56	303/0529	303/0543
57	303/0616	303/0656
58	303/0724	303/0809
59	303/0853	303/0936
60	303/1000	303/1042
61	303/1110	303/1156
62	303/1220	303/1306
63	303/1328	303/1415
64	303/1436	303/1524
65	303/1543	303/1636
66	303/1650	303/1728
67	303/1813	303/1859
68	303/1932	303/2015
69	303/2050	303/2137
70	304/0212	302/0310
71	304/0321	304/0436
72	304/0450	304/1548
73	304/0837	304/1202
74	304/1221	304/1602
75	304/1618	304/2000

PGC97007

Line	Start Time	End Time
1	219/0450	219/1218
2	219/1352	219/1410
3	219/1424	219/1441
4	219/1441	219/1514
5	219/1519	219/1532
6	219/1544	219/1600
7	220/0320	220/0656
8	220/0802	220/1125
9	220/1245	220/1455
10	221/0228	221/0500
11	221/0556	221/1119
12	221/1205	221/1447
13	221/1456	221/1656
14	221/2246	222/0754
15	222/0805	222/1034
16	222/1205	222/1633
17a	222/2319	223/0150
18	223/0235	223/0256
17b	223/0332	223/0645
19	223/0715	223/1129
20	223/1200	223/1633
21	223/1640	223/1904
12b	223/1927	223/2312
22	223/2358	224/0452
23	224/0532	224/0650
24	224/0654	224/1100
25	224/1147	224/1533
26	225/0130	225/0403
27{1}	225/0424	225/0829
28	225/0850	225/1032
29	225/1120	225/1542
30	226/0227	226/0748
31	226/0748	226/0834
32	226/0834	226/1309
33	226/1316	226/1602
34	226/1611	226/1801
35	227/0522	227/0816
36	227/0906	227/1218
37	227/1220	227/1300
38	227/2136	227/2300
39	227/2318	228/0045
40	228/0054	228/0300
41	228/0327	228/0535
42	228/0535	228/0647
43	228/0659	228/0816
44	228/0956	228/1215
45	228/1239	228/1354
46A	228/1418	228/1523
46B	228/1609	228/1738

Table 2: Multichannel and Single Channel Seismic Lines

PGC96006

Line	Start Time	End Time	Start Shot	End Shot	Tape
1	290/2130	291/0650	1187	4558	1,2,3
2	291/0700	291/1536	4874	8295	3,4
3A	291/1602	291/1911	8304	9455	4
3B	292/0511	292/1217	9456	12287	5
4	292/1302	292/2122	12297	15856	5
5A	292/2200	293/0617	16032	19265	6
6	293/0700	293/1718	19560	23627	6
7	293/2030	294/0634	24129	28412	7
8A	294/0738	294/1043	28653	30097	7
9A	294/1143	294/1546	30223	31927	7,8
10	294/1604	294/1734	31929	32573	8
11	294/1836	295/0458	32576	36927	8
8B	295/0531	295/1311	37156	40404	8,9
9B	295/1437	295/2137	40409	43365	9
12	295/2213	296/0043	43370	44420	9
13	296/0058	296/0332	44422	45415	10
14	296/0348	296/1041	45418	48368	10
15	296/1202	296/1636	48369	50313	10
16	296/1711	296/1834	50329	50910	10
17	296/1900	296/2149	50966	52360	10
18	296/2152	296/2325	52362	52998	11
19	296/2335	297/0809	53071	56579	11
20	297/0809	297/0836	56580	56765	11
21	297/0836	297/1919	56766	51510	11,12
22	297/2019	297/2349	61511	62999	12
23	298/0015	298/0344	63002	64488	12
24	298/0408	298/0717	64677	66069	12
25	298/0800	298/1032	66070	67371	12
26	298/1039	298/1243	67372	68291	13
27	298/1258	298/1310	68202	68369	13
28	299/0130	299/0906	68403	72004	13
29	299/0938	299/1220	72005	73246	13
30	299/1252	2991329	73247	73440	13
31	299/1408	299/1440	73441	73669	13
32	299/2209	300/0703	73661	77953	13,14
33	300/0841	300/1706	77956	81597	14
34	301/0209	301/0608	81599	83113	14,15
35	301/0615	301/1036	83114	85116	15
36	301/1050	301/1217	85117	85787	15
37	301/1221	301/1819	85788	88258	15
46	302/1113	302/1530	88267	90327	16
70	304/0212	302/0310	90331	90758	16
71	304/0321	304/0436			
72	304/0450	304/1548			
73	304/0837	304/1202	90760	92313	16
74	304/1221	304/1602	92315	92696	16
75	304/1618	304/2000	94008	95525	16

Table 2 cont'd

PGC97007

Line	Start Time	End Time	Start Shot	End Shot	Tape
10	221/0228	221/0500	0	3855	2
11	221/0556	221/1119	5386	14303	2
12	221/1205	221/1447	15477	20067	2
13	221/1456	221/1656	20485	23920	2
14	221/2246	222/0754	96	14130	3
15	222/0805	222/1034	14478	18742	3
16	222/1205	222/1633	21146	274	3,4
17a	222/2319	223/0150	320	3950	4,5
17b	223/0332	223/0645	5336	10145	5
19	223/0715	223/1129	215	7602	5
20	223/1200	223/1633	8355	15956	5
21	223/1640	223/1904	16160	20100	5
12b	223/1927	223/2312	20746	27288	5
22	223/2358	224/0452	28681	36938	5
23	224/0532	224/0649	37882	39906	6
24	224/0624	224/1059	40005	47406	6
25	224/1147	224/1533	48830	55621	6
26	225/0130	225/0403	798	4879	6
27	225/0424	225/0822	5404	12081	6
28	225/0850	225/1032	12744	15657	6
29	225/1120	225/1542	17041	24376	6
30	226/0524	226/0748	1470	5307	7
31	226/0748	226/0834	5308	6589	7
32	226/0834	226/1309	6590	2129	8
33	226/1316	226/1602	2278	7232	8
34	226/1611	226/1801	7504	10648	8
35	227/0522	227/0817	269	5101	9
36	227/0906	227/1220	6488	11657	9
37	227/1220	227/1300	11742	12710	9
38	227/2136	227/2300	53	2271	10
39	227/2318	228/0045	348	2053	10
40	228/0054	228/0300	2237	4943	10
41	228/0327	228/0535	5523	8104	10
42	228/0535	228/0647	8105	9562	10
43	228/0659	228/0816	9801	11373	10
44	228/0956	228/1215	1054	1651	10
45	228/1239	228/1354	1652	1992	10
46B	228/1609	228/1738	2304	2735	10
46A	228/1418	228/1523	1997	2299	10

Table 3: Huntec Lines

PGC96006

Line	Start Time	End Time	Tapes
1	290/2133	291/0609	1,2
2	291/0641	291/1536	2,3
3A	291/1602	291/1911	3
3B	292/0511	292/1217	3
4	292/1301	292/2122	3,4,5
5A	292/2154	293/0607	5,6,7
6	293/0657	293/1815	7,8,9
7	293/2015	294/0634	9
8A	294/0739	294/1043	10
9A	294/1145	294/1546	10
10	294/1604	294/1734	10
11	294/1848	295/0458	11
8B	295/0531	295/1311	11,12
9B	295/1438	295/2137	12
12	295/2213	296/0043	12
13	296/0059	296/0330	13
14	296/0338	296/1041	13
15	296/1202	296/1636	13
16	296/1711	296/1835	13
17	296/1844	296/2149	13
18	296/2153	296/2327	13
19	296/2337	297/0809	14
20	297/0809	297/0836	14
21	297/0836	297/1919	14
22	297/2019	297/2351	15
23	298/0015	298/0346	15
24	298/0406	298/0717	15
25	298/0800	298/1036	15
26	298/1036	298/1243	15
27	298/1258	298/1310	15
28	299/0130	299/0906	16
29	299/0938	299/1220	16
30	299/1300	2991320	16
31	299/1408	299/1441	16
32	299/2209	300/0700	16
33	300/0841	300/1706	17
34	301/0207	301/0609	17
35	301/0615	301/1036	17
36	301/1042	301/1216	17
37	301/1221	301/1836	17
40	302/0320	302/0342	18
46	302/1114	302/1530	18
47	302/1554	302/1634	18
48	302/1634	302/1641	18
49	302/1641	302/1708	18
50	302/1708	302/1732	18
51	302/1732	302/1801	18
52	302/1801	302/1828	18
53	302/1828	302/1927	18
54	302/1927	302/1951	18
55	302/1951	302/?	18

PGC97007

Line	Start Time	End Time	Tapes
10	221/0228	221/0500	2
11	221/0556	221/1119	2
12	221/1205	221/1447	2
13	221/1456	221/1656	2
14	221/2246	222/0754	3
15	222/0805	222/1034	3
16	222/1205	222/1633	3,4
17a	222/2319	223/0150	4,5
17b	223/0332	223/0645	5
19	223/0715	223/1129	5
20	223/1200	223/1633	5
21	223/1640	223/1904	5
12b	223/1927	223/2312	5
22	223/2358	224/0452	5
23	224/0532	224/0649	6
24	224/0624	224/1059	6
25	224/1147	224/1533	6
26	225/0130	225/0403	6
27	225/0424	225/0822	6
28	225/0850	225/1032	6
29	225/1120	225/1542	6
30	226/0524	226/0748	7
31	226/0748	226/0834	7
32	226/0834	226/1309	8
33	226/1316	226/1602	8
34	226/1611	226/1801	8
35	227/0522	227/0817	9
36	227/0906	227/1220	9
37	227/11742	227/12710	9
38	227/2136	227/2300	10
39	227/2318	228/0045	10
40	228/0054	228/0300	10
41	228/0327	228/0535	10
42	228/0535	228/0647	10
43	228/0659	228/0816	10
44	228/0956	228/1215	10
45	228/1239	228/1354	10
46B	228/1609	228/1738	10
46A	228/1418	228/1523	10

Table 4: PGC96006 Sidescan Sonar Lines

Line	Start Time	End Time	Tapes	File Numbers
38	302/0049	302/0126	18	1
39	302/0142	302/0219	18	3
41	302/0504	302/0529	18	5
42	302/0613	302/0647	18	6-7
43	302/0851	302/0918	18	8
44	302/0930	302/1000	18	9
45	302/1016	302/1041	18	10
56	303/0529	303/0543	19	1
57	303/0616	303/0656	19	2
58	303/0724	303/0809	19	3
59	303/0853	303/0936	19	4
60	303/1000	303/1042	20	1
61	303/1110	303/1156	20	2
62	303/1220	303/1306	21	1
63	303/1328	303/1415	21	2
64	303/1436	303/1524	21	3
65	303/1543	303/1636	21	4-6
66	303/1650	303/1728	21	7
67	303/1813	303/1859	21	8
68	303/1932	303/2015	21	9
69	303/2050	303/2137	21	10

Table 5: Core Locations

PGC96006

Core	Time (UTC)	Lat (WGS84)	Long (WGS84)	Length	Type
TUL96B001	298/1605	48° 11.734'	-123° 40.663'	121 cm	Piston
TUL96B002	298/1739	48° 11.725'	-123° 40.486'	164 cm	Piston
TUL96B003	298/1854	48° 22.01'	-123° 29.275'	376 cm	Piston
TUL96B004	299/1605	48° 17.01'	-122° 50.05'	363 cm	Piston
TUL96B005	299/1742	48° 16.988'	-122° 50.206'	583 cm	Piston
TUL96B006	299/1942	48° 16.983'	-122° 50.337'	565 cm	Piston
TUL96B007	299/2049	48° 16.97'	-122° 50.61'	347 cm	Piston
TUL96B008	300/1835	48° 22.99'	-122° 47.27'	403 cm	Piston
TUL96B009	300/1957	48° 23.006'	-122° 52.864'	370 cm	Piston
TUL96B010	300/2151	48° 18.008'	-123° 06.34'	19 cm	Piston
TUL96B011	300/2250	48° 17.984'	-123° 06.402'	26 cm	Piston
TUL96B012	301/0113	48° 24.08'	-123° 23.64'	203 cm	Piston
TUL96B013	301/2052	48° 17.087'	-123° 27.855'	----	Piston
TUL96B014	301/2200	48° 23.00'	-123° 12.52'	204 cm	Piston
TUL96B015	301/2355	48° 22.97'	-123° 13.93'	----	Piston
TUL96B016	305/1545	48° 35.41'	-123° 30.31'	432 cm	Gravity
TUL96B017	305/1714	48° 37.97'	-123° 30.09'	295 cm	Gravity

PGC97007

Core Number	Time(Z)	Lat (NAD83)	Long (NAD83)	Length (cm)	Type
TUL97B001	218/1642	48° 24.991'	123° 25.785'	263 cm	piston
TUL97B002	218/1825	48° 24.921'	123° 25.578'	236 cm	piston
TUL97B003	218/2014	48° 24.588'	123° 24.999'	370 cm	piston
TUL97B004	219/1646	48° 22.97'	122° 47.33'	448 cm	piston
TUL97B005	219/1930	48° 21.484'	122° 59.425'	513 cm	piston
TUL97B006	219/2315	48° 21.374'	122° 59.470'	319 cm	piston
TUL97B007	220/1617	48° 13.993'	123° 10.092'	165 cm	piston
TUL97B008	220/1736	48° 16.972'	123° 10.544'	347 cm	piston
TUL97B009	220/1934	48° 17.984'	123° 03.104'	457 cm	piston
TUL97B010	220/2040	48° 17.999'	123° 03.858'	59 cm	piston
TUL97B011	220/2139	48°.17.996'	123° 02.381'	lost;washed	piston
TUL97B012	221/1830	48° 23.97'	123° 24.817'	373 cm	piston
TUL97B013	221/2058	48° 20.005'	123° 30.785'	93 cm	piston
TUL97B014	222/1919	48° 23.511'	122° 44.223'	86 cm	piston
TUL97B015	222/2036	48° 20.932'	122° 48.539'	483 cm	piston
TUL97B016	222/2148	48° 20.943'	122° 48.477'	511 cm	piston
TUL97B017	224/1752	48° 25.153'	122° 56.416'	110 cm	piston
TUL97B018	224/2042	48° 16.744'	122° 54.042'	337 cm	piston
TUL97B019	224/2137	48° 17.024'	122° 53.909'	54 cm	piston
TUL97B020	224/2257	48° 14.018'	122° 48.093'	69 cm	piston
TUL97B021	225/1759	48° 20.158'	122° 57.236'	383 cm	piston
TUL97B022	225/2329	48° 22.983'	123° 13.967'	no recovery	vibro
TUL97B023	226/2042	48° 20.013'	122° 30.780'	131 cm	vibro
TUL97B024	226/2236	48° 22.973'	123° 14.025'	1 bag	vibro
TUL97B025	226/2258	48° 22.990'	123° 14.099'	153 cm	vibro
TUL97B026	226/2330?	48° 22.971'	123° 13.972'	1 dixie cup	vibro

Table 6: Radiocarbon (AMS) ^{14}C data

CAMS #	Sample Name	Depth (cm)	Ident	$\delta^{13}C$	fraction Modern	±	$D^{14}C$	±	^{14}C age	±
58672	T9603-1-20	20	Macoma lipara	-0.3	0.8069	0.0040	-193.1	4.0	1720	40
58673	T9603-3-98	360	Nucula tenuis	0	0.2272	0.0012	-772.8	1.2	11900	50
58674	T9604-2-6	63	Polinices pallidus	0	0.8626	0.0042	-137.4	4.2	1190	40
58675	T9604-3-110	319	Macoma brota	0	0.3552	0.0018	-644.8	1.8	8310	50
58676	T9605-1-63	63	Compsomyax subdiaphana	0	0.3435	0.0015	-656.5	1.5	8580	40
58677	T9605-2-70	210	Yoldia martyria	0	0.2663	0.0014	-733.7	1.4	10630	50
58678	T9605-3-93	373	Compsomyax subdiaphana	0	0.2614	0.0014	-738.6	1.4	10780	50
58679	T9606-1-85	85	Yoldia martyria	0	0.2644	0.0014	-735.6	1.4	10690	50
58680	T9606-4-68	479	bivalve fragment	0	0.2567	0.0016	-743.3	1.6	10930	50
58681	T9607-2-29	64	Macoma brota	0	0.1889	0.0012	-811.1	1.2	13390	60
58682	T9702-1-31	31	wood	-25	0.9769	0.0049	-23.1	4.9	190	50
58683	T9702-1-45	45	Compsomyax subdiaphana	0.2	0.8726	0.0043	-127.4	4.3	1090	40
58684	T9702-2-10	96	Macoma brota	0	0.2659	0.0015	-734.1	1.5	10640	50
58685	T9702-2-138	224	Macoma lipara	0	0.2924	0.0015	-707.6	1.5	9880	50
58686	T9704-1-13	13	shell fragments	0	0.6339	0.0031	-366.1	3.1	3660	40
58687	T9705-2-64	114	shell fragments	0	0.2560	0.0015	-744.0	1.5	10950	50
58688	T9705-2-73	123	Cyclocardia ventricosa	0	0.2664	0.0012	-733.6	1.2	10630	40
58689	T9705-3-17	205	Macoma brota	0	0.1926	0.0012	-807.4	1.2	13230	50
58690	T9707-1-31	31	Macoma lipara	0	0.1922	0.0011	-807.8	1.1	13250	50
58691	T9708-1-33	33	Chlamys rubida	0	0.5840	0.0031	-416.0	3.1	4320	50
58692	T9709-1-93	93	Nuculana fossa	0.6	0.1921	0.0012	-807.9	1.2	13250	50
58693	T9709-1-133	133	fish jawbone	0	0.2066	0.0012	-793.4	1.2	12670	50
58694	T9711-2-37	182	Nuculana fossa	0	0.1870	0.0012	-813.0	1.2	13470	60
58695	T9712-3-23	246	Mya truncata	0	0.2632	0.0017	-736.8	1.7	10720	60
58696	T9712-3-102	325	Macoma calcarea	0	0.1818	0.0011	-818.2	1.1	13690	50
58697	T9716-1-43	43	Balanus cariosus	0	0.7319	0.0038	-268.1	3.8	2510	50
58698	T9716-2-120	179	Cyclocardia ventricosa/Compsomyax subdiaphana	0	0.2271	0.0013	-772.9	1.3	11910	50
58699	T9716-2-133	192	serpulid worm tube fragment	0	0.1974	0.0011	-802.6	1.1	13030	50
58700	T9716-3-130	342	serpulid worm tube fragment	0	0.1945	0.0012	-805.5	1.2	13150	50
58701	T9716-4-142	504	Nuculana fossa	0	0.1863	0.0011	-813.7	1.1	13500	50
58702	T9718-2-23	61	neogastropod	0	0.3125	0.0016	-687.5	1.6	9340	50
58703	T9718-3-23	206	Ophiodermella cancellata	0	0.3054	0.0016	-694.6	1.6	9530	50

58704	T9718-3-137	320	Chlamys rubida	0.4	0.2936	0.0015	-706.4	1.5	9840	50
58705	T9721-2-137	221	Pododesmus macroschisma	1.2	0.2680	0.0014	-732.0	1.4	10580	50

1) Delta ^{13}C values are the assumed values according to Stuiver and Polach (Radiocarbon, v. 19, p.355, 1977) when given without decimal places. Values measured for the material itself are given with a single decimal place.

2) The quoted age is in radiocarbon years using the Libby half life of 5568 years and following the conventions of Stuiver and Polach (ibid.).

3) Radiocarbon concentration is given as fraction Modern, $D^{14}C$, and conventional radiocarbon age.

4) Sample preparation backgrounds have been subtracted, based on measurements of samples of ^{14}C-free coal and calcite. Backgrounds were scaled relative to sample size.

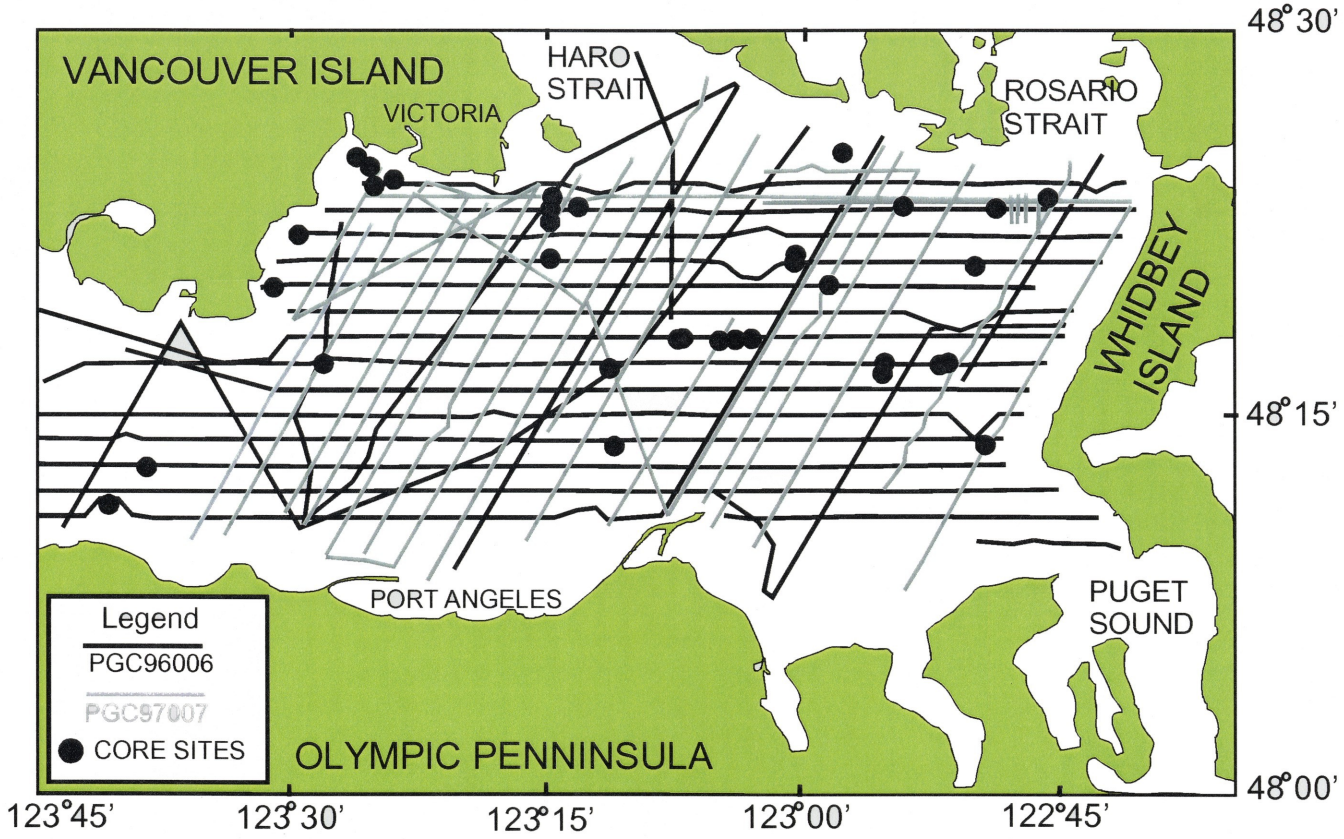

Figure 1: Cruise track and core locations for PGC96006 and PGC97007 (see Tables 1-5).

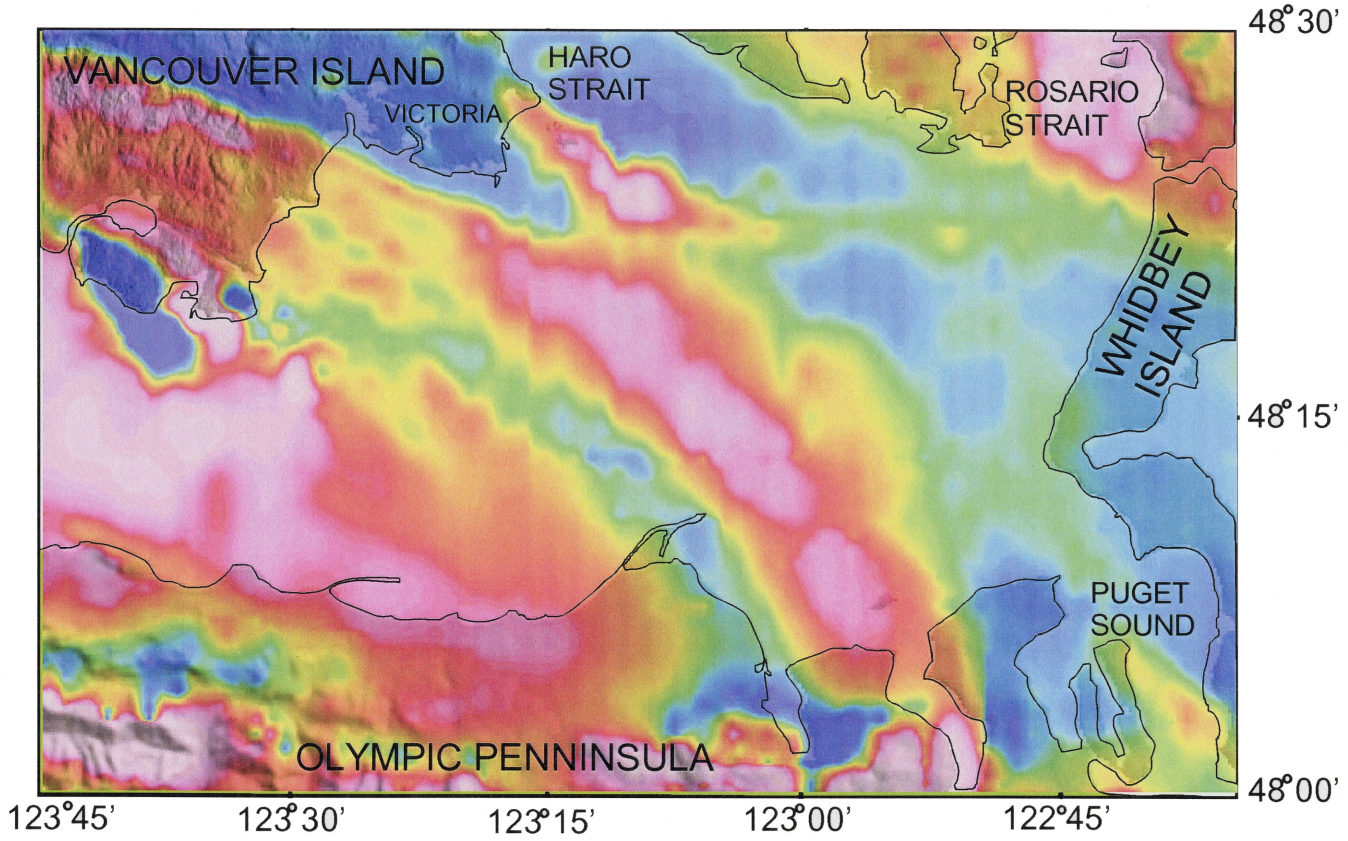

Figure 2: Airborne magnetic data over the study region.

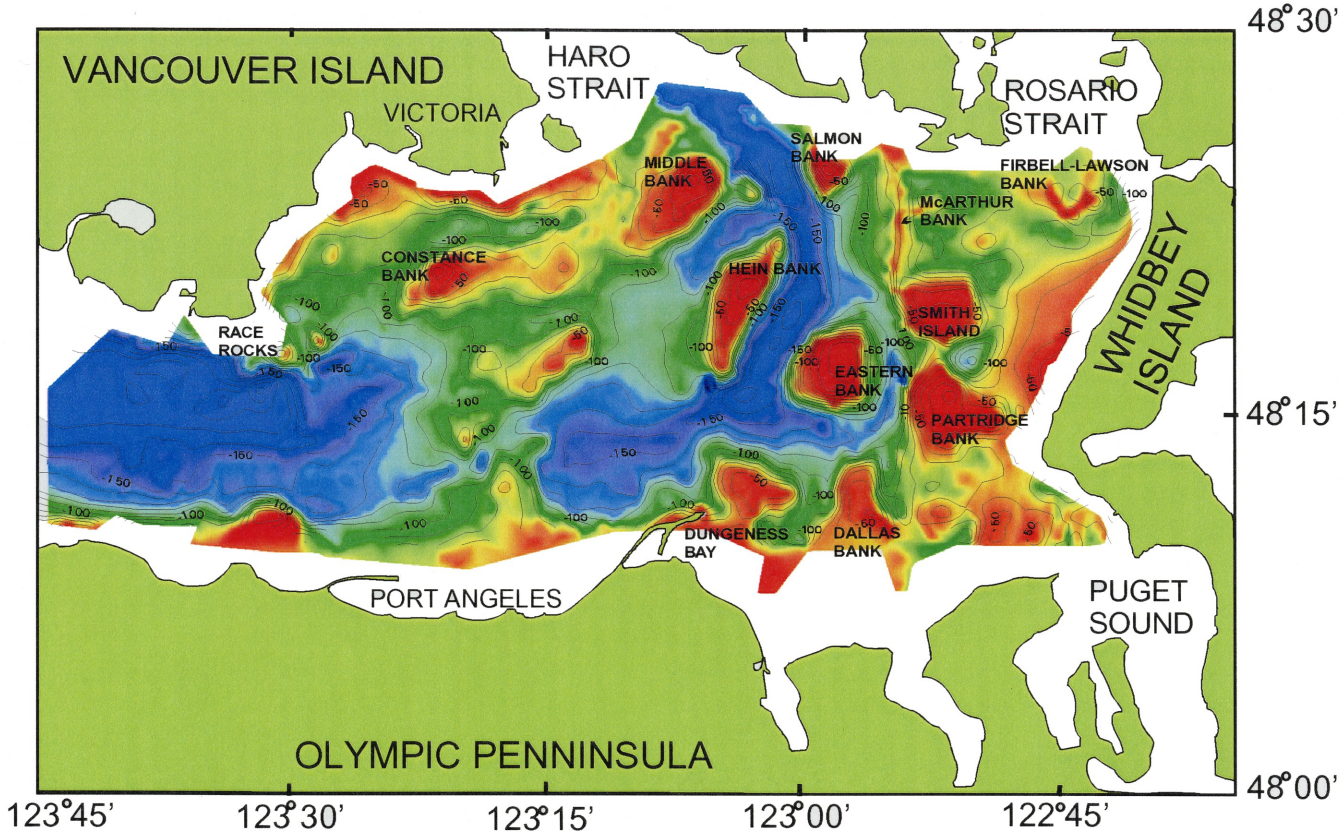

Figure 3: Bathymetry of the study region.

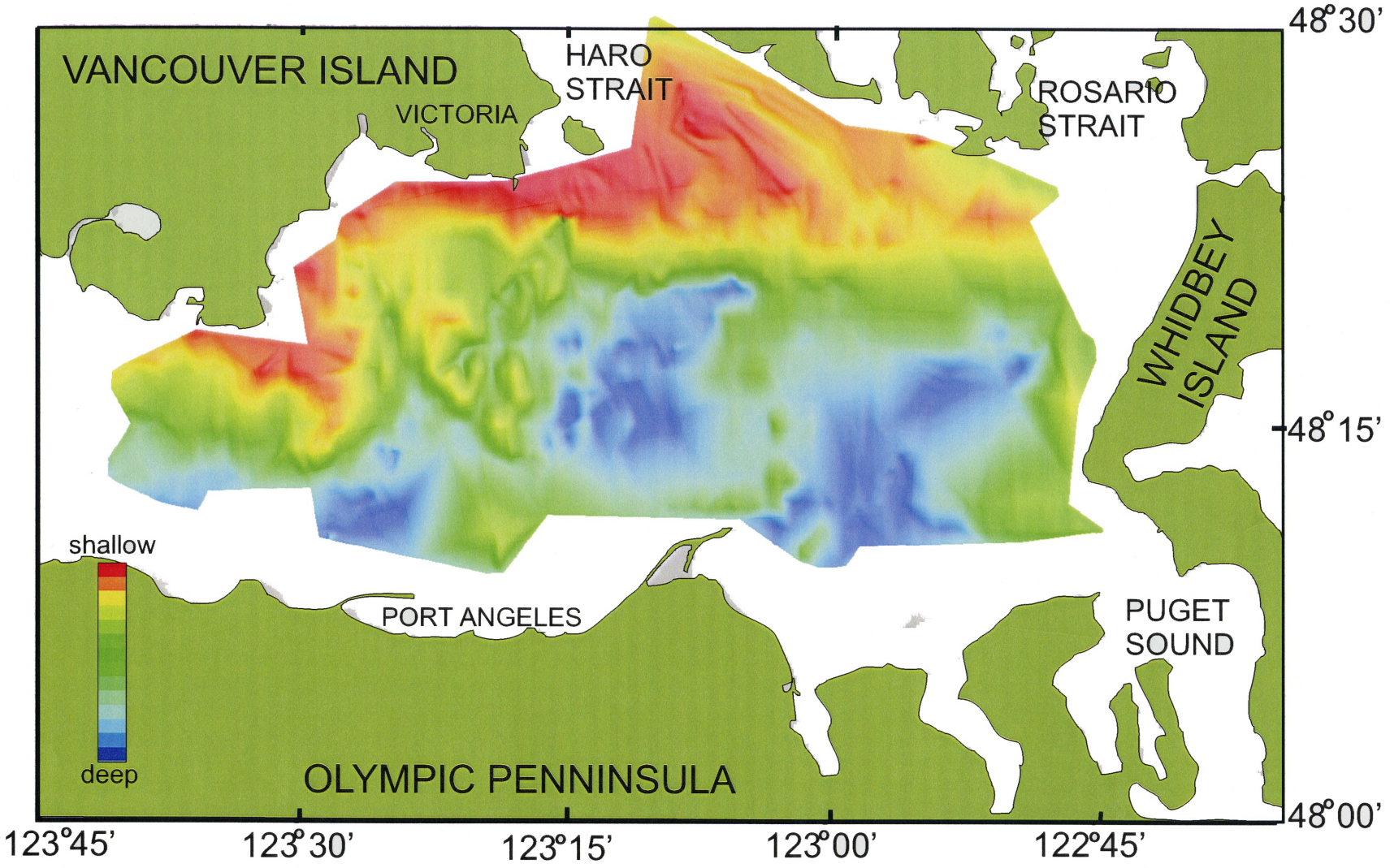

Figure 4: Depth to the Base of the Quaternary, derived from digital horizon picking of seismic data

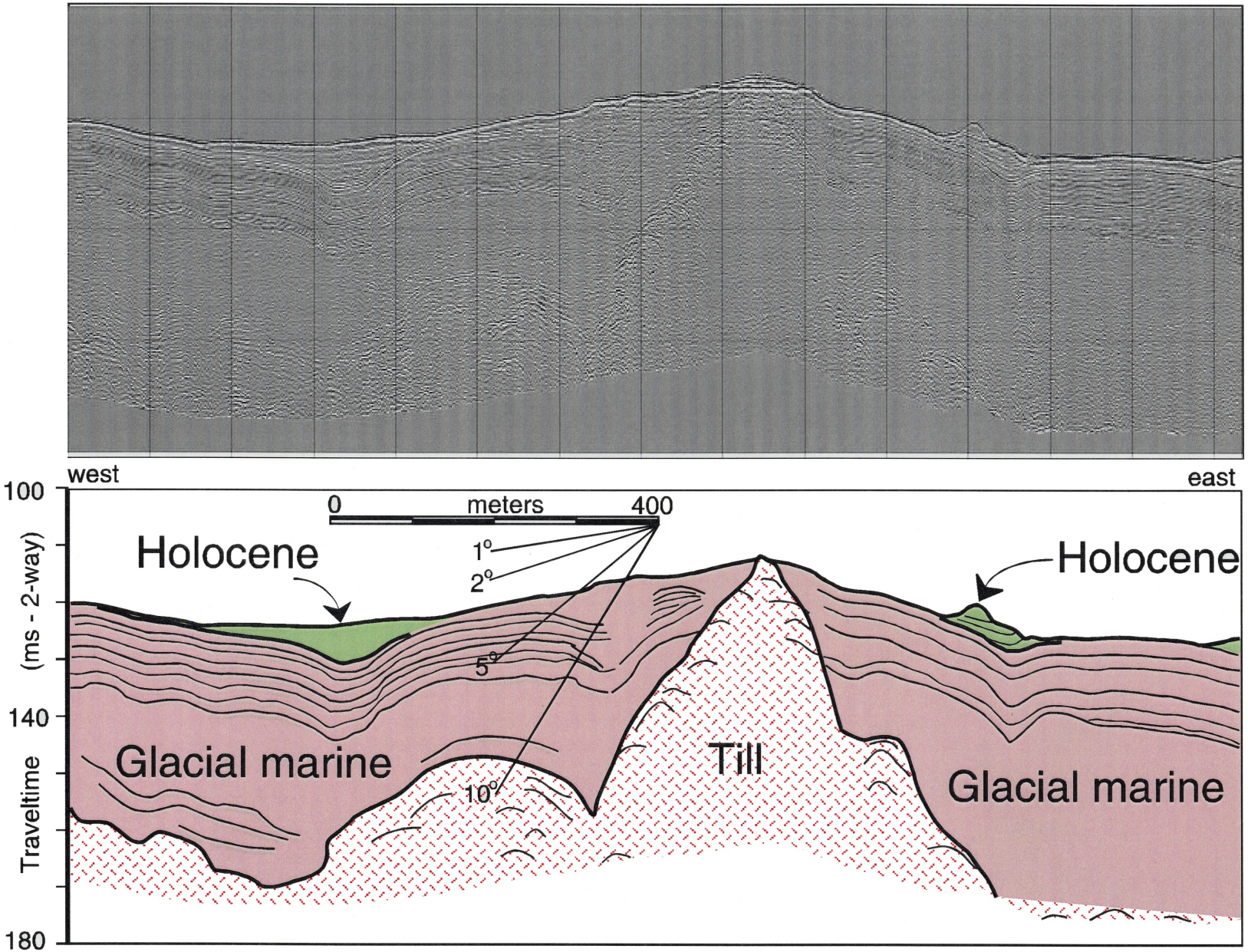

Figure 5: Huntec DTS profile showing representatives of the three seismic units above bedrock: diamict or till, glacial marine sediments and Holocene reworked material

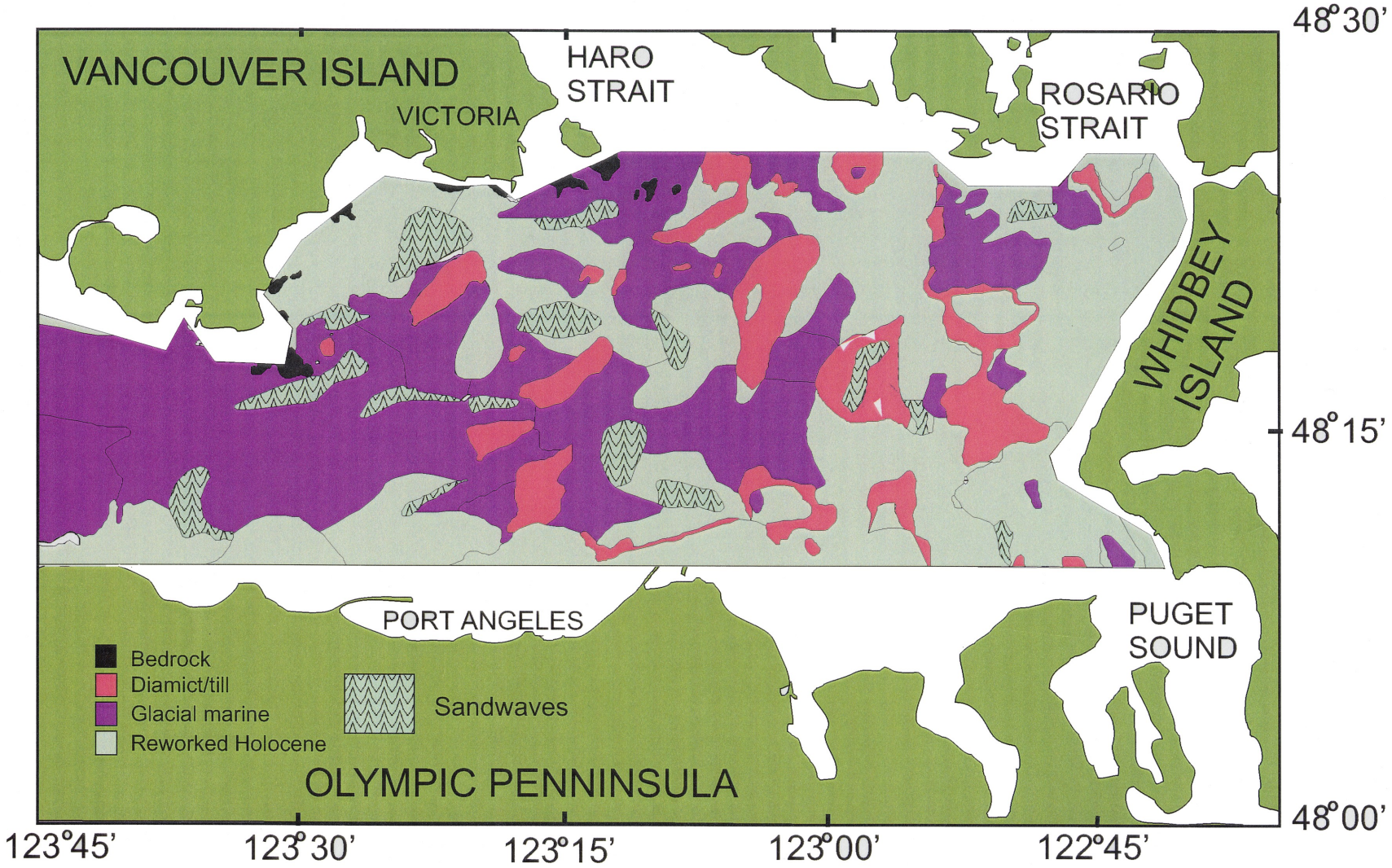

Figure 6 Surficial geology map based on the interpretation of Huntec boomer high resolution seismic reflection data and piston cores. The map represents outcropping at the seafloor of these units.

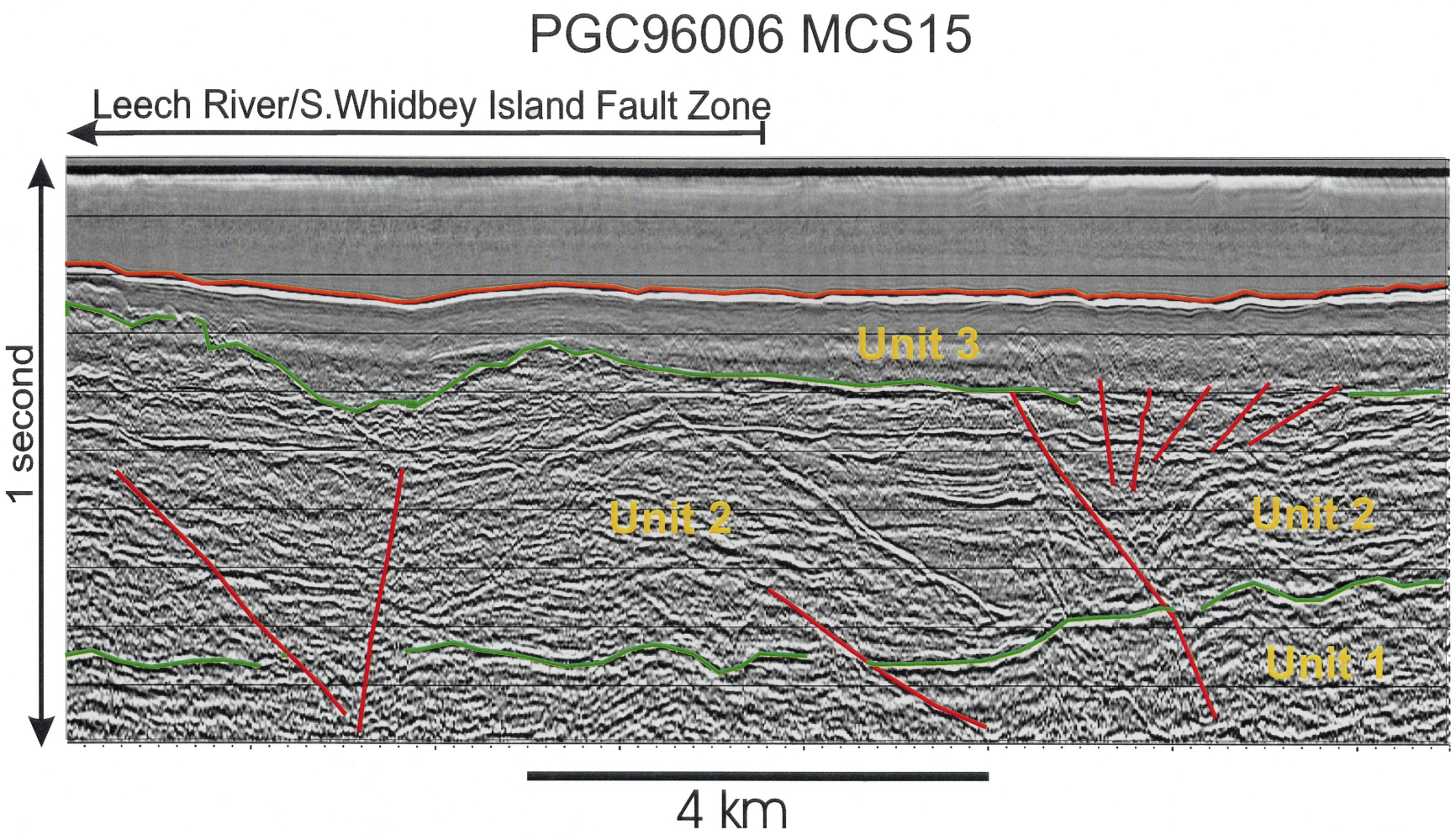

Figure 7 Multichannel seismic reflection line 15 across the Leech River/South Whidney Island fault zone. The image shows mostly Quaternary sediments, with fault offsets mapped with red line. Unit 2 (till and diamict) is complex as it probably represents till or diamict remnant from a number of Quaternary glaciations.

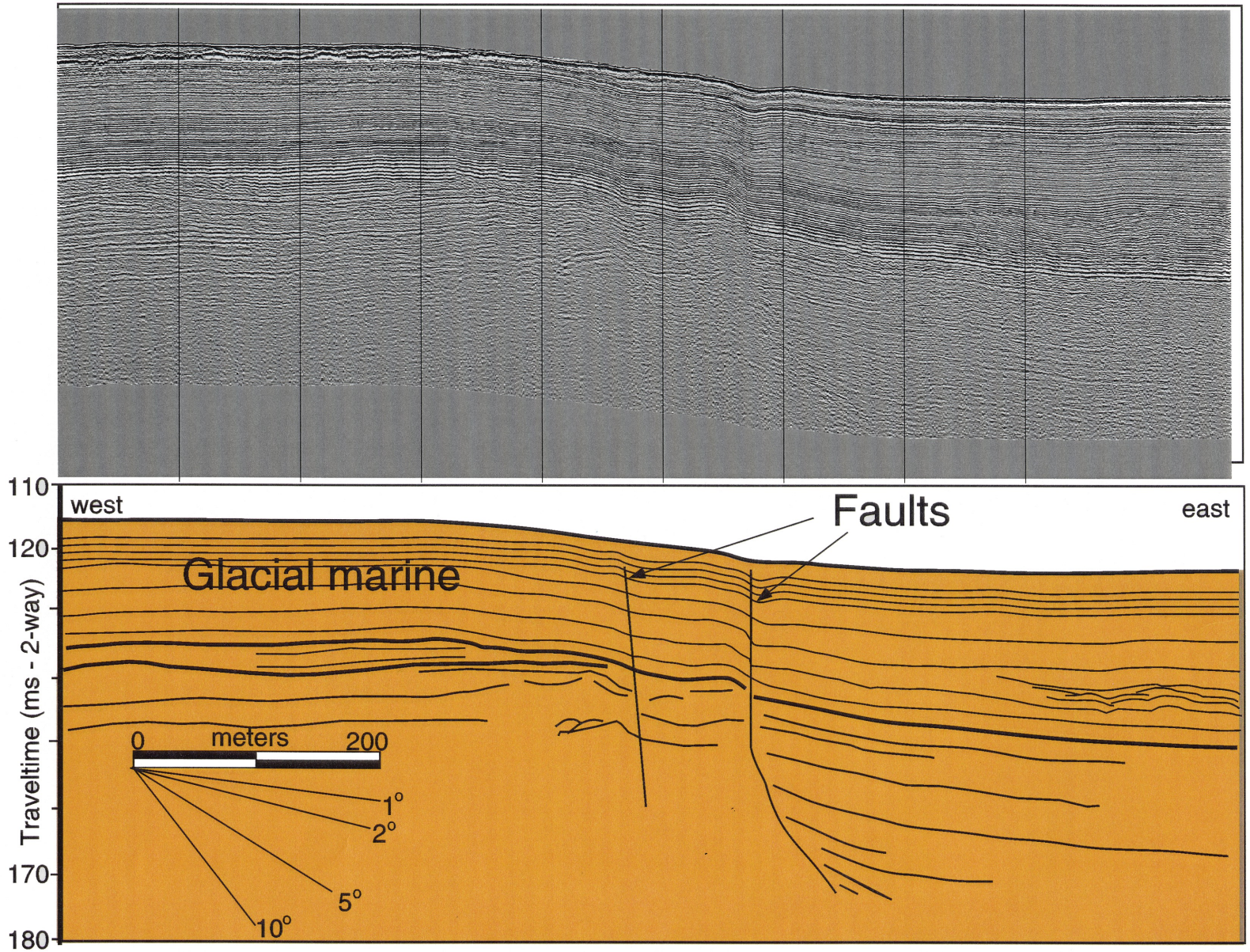

Figure 8 Huntec DTS high resolution seismic reflection profile showing offset reflectors within Unit 3, penetrating to the seafloor with bathymetric expression.

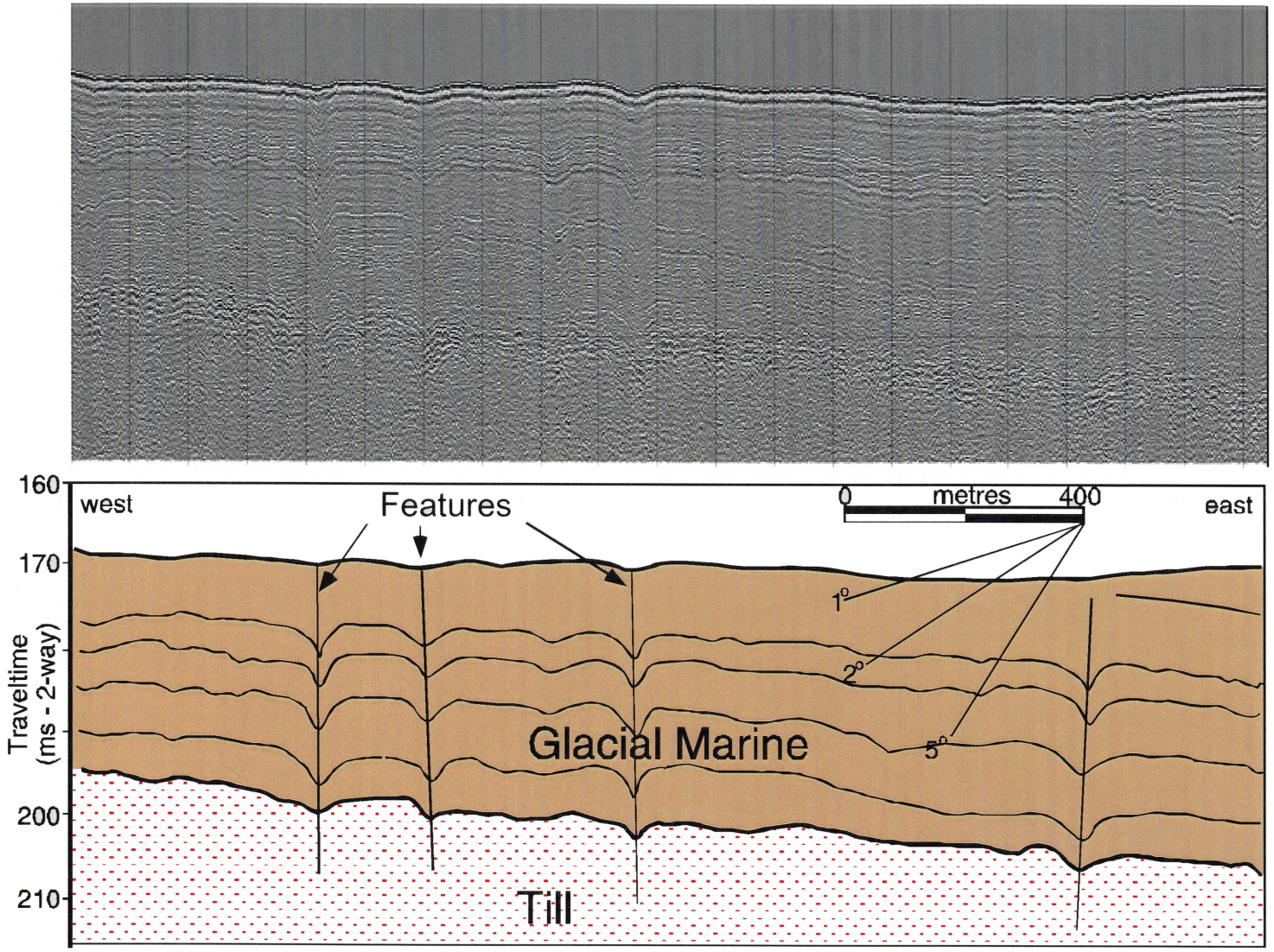

Figure 9 Huntec DTS high resolution seismic reflection profile showing sediment deformation features (downdrops). These features are believed to represent liquifaction pipes, as seen in outcrop along Whidbey Island, which, in all probability are related to ground acceleration due to earthquakes. In many examples, these deformation features reach to the seafloor and have a bathymetric expression associated with them.

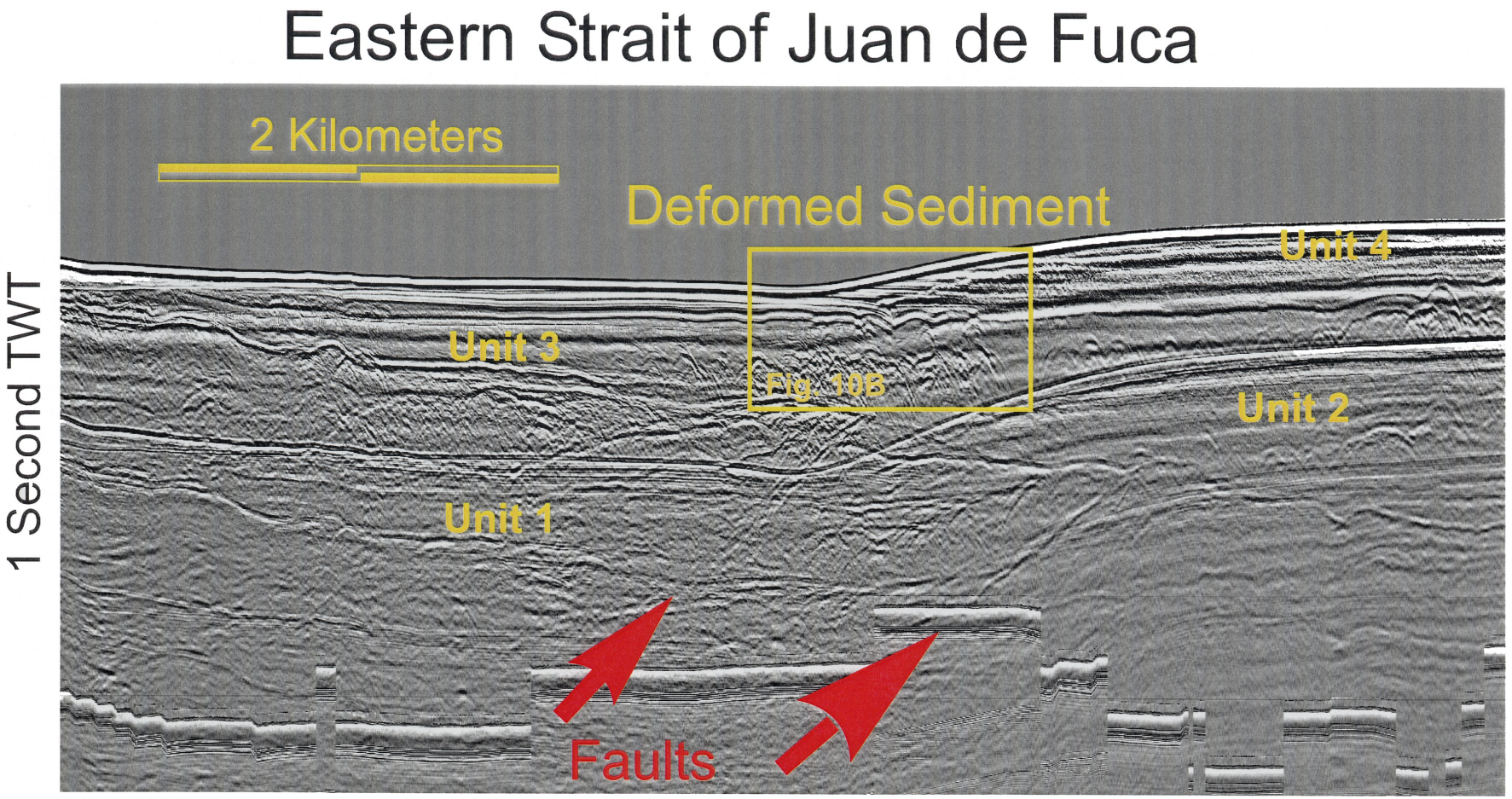

Figure 10A Single channel seismic reflection line showing basement offset reflectors, with sediment deformation features above (see Fig. 10B).

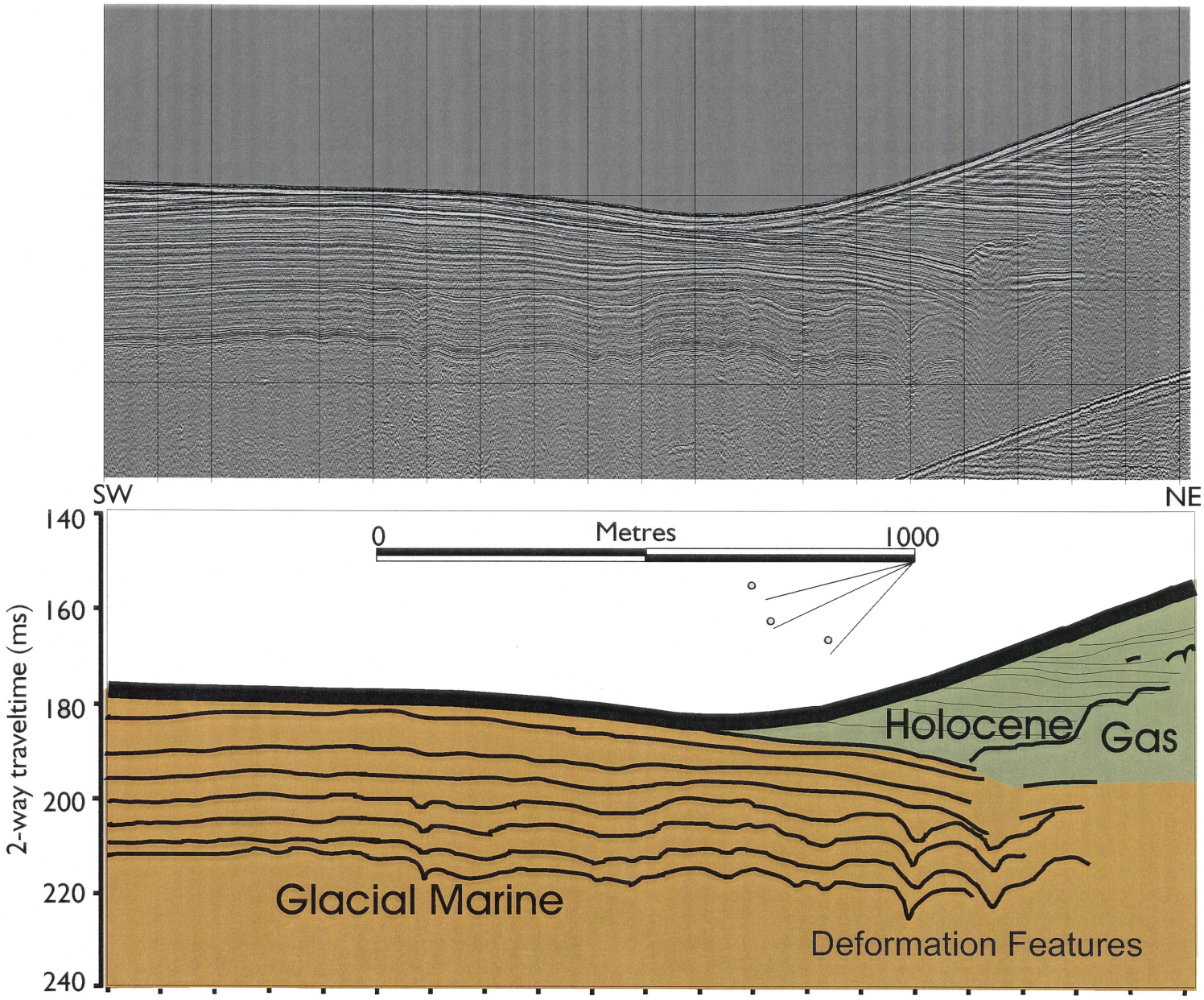

Figure 10B Huntec DTS boomer seismic reflection profile showing sediment deformation features which are over top of faults recognized in the deeper seismic profiles (Fig. 10A). These deformation features have been buried by subsequent Holocene deposition.

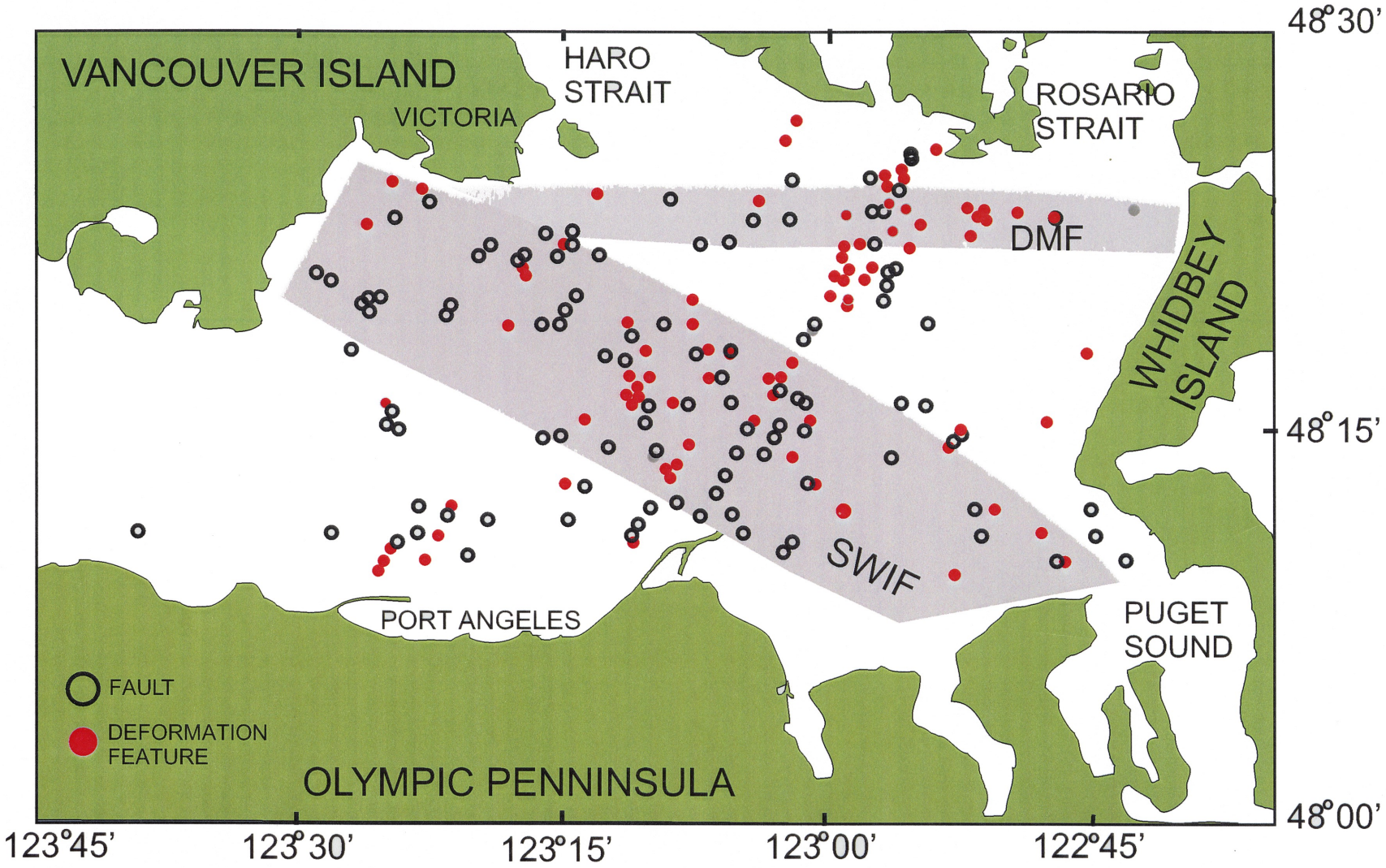

Figure 11 Distribution of faults and sediment deformation features from interpretation of seismic reflection profiles. The grey areas represent broad zones of faulting and deformation which correlate with the Leech River/South Whidbey Island fault (SWIF) zone and the Devil's Mountain fault zone (DMF).